Nucleic Acids Research, 1998, Vol. 26, No. 16 **3707–3716**

Mutational analysis of exoribonuclease I from *Saccharomyces cerevisiae*

Andrew M. Page[+], Kristina Davis, Catherine Molineux, Richard D. Kolodner[§] and Arlen W. Johnson*

Department of Microbiology and the Institute for Cellular and Molecular Biology, University of Texas at Austin, Austin, TX 78712-1095, USA

Received May 8, 1998; Revised and Accepted June 25, 1998

ABSTRACT

Exoribonuclease I from yeast is a 175 kDa protein that is responsible for the majority of cytoplasmic mRNA degradation. Alignment of the Xrn1p sequence with homologs from yeast as well as from higher eukaryotes suggests that the protein is composed of several domains: two acidic N-terminal domains which likely contain the exonuclease, a basic middle domain and a basic C-terminal domain. Deletion analysis demonstrated that the C-terminus is dispensable for most *in vivo* and *in vitro* functions but confers a dominant negative growth inhibition when expressed at high levels. This growth inhibition is not due to the exonuclease function of the protein. To identify specific residues responsible for *in vivo* function, a screen was carried out for non-complementing missense mutations. Fourteen single point mutations were identified that altered highly conserved amino acids within the first N-terminal domain of Xrn1p. All of the mutations reduced exonuclease activity measured *in vivo* and *in vitro* using affinity-purified proteins. The mutants fell into two phenotypic classes, those that reduced or abolished exonuclease activity without qualitatively changing the products of RNA degradation and those that gave rise to novel degradation intermediates on certain RNAs.

INTRODUCTION

XRN1 encodes a 175 kDa exoribonuclease that is responsible for the majority of cytoplasmic mRNA turnover in yeast, including general deadenylation-dependent (1; reviewed in 2) as well as nonsense-mediated, deadenylation-independent degradation (3). *xrn1* deletion mutants are viable, but grow slowly (1,4) and accumulate decapped deadenylated mRNAs (5–7). Xrn1p also degrades internal transcribed spacer I (ITSI), a product of rRNA processing, indicating that its activity is not restricted to mRNAs (8). Although highly specific for RNAs containing 5′-PO_4 (9), the exonuclease shows little sequence specificity, suggesting that the enzyme can act on a broad range of substrates. However, certain RNA structural elements, such as stable hairpins and poly(G) tracts, inhibit degradation by Xrn1p (10,11).

The enzyme hydrolyzes RNA in a 5′→3′ direction yielding mononucleotides (9), although the initial cleavage product may be a short oligonucleotide (12). Such a 5′-exoribonuclease has not been identified from prokaryotic organisms and sequence alignments comparing the Xrn1p protein sequence with translated genome sequences of eubacteria or archaebacteria have not revealed any apparent homologs. On the other hand, Xrn1p appears to be highly conserved throughout eukaryotes. Homologs of Xrn1p have been identified and characterized from *Schizosaccharomyces pombe* (13), *Drosophila melanogaster* (D.Till, B.Linz, J.Seago, J.McClellan, J.McCarthy and S.F.Newbury, personal communication) and mouse (14,15) and immuno-cross-reactive proteins have been identified from additional species (16). A second 5′-exoribonuclease from *Saccharomyces cerevisiae*, Rat1p, shares considerable homology with Xrn1p and is required for RNA degradation or processing in the nucleus (17). Rat1p is also conserved throughout eukaryotes (18,19). Xrn1p and Rat1p are functionally interchangeable exoribonucleases, but are normally restricted to and required in the cytoplasm and nucleus respectively (17).

xrn1 mutants and the Xrn1 protein have been identified using a variety of genetic and biochemical approaches and *XRN1* has also been referred to as *KEM1*, *SEP1*, *DST2*, *RAR5 SKI1* and *DST2* (4,9,20,21). However, the localization of Xrn1p to the cytoplasm appears to restrict the possible functions of Xrn1p to cytoplasmic events, primarily RNA degradation. It has also been suggested that Xrn1p is a tubulin binding protein (22), based on the hypersensitivity of *xrn1* mutants to the tubulin destabilizing drug benomyl (4), the ability of Xrn1p to facilitate tubulin polymerization *in vitro* and a genetic interaction with tubulin mutants (22). A screen for mutations lethal in combination with an *xrn1* deletion mutation identified mutations in *SKI2* and *SKI3* (23), which suppress expression of poly(A)$^-$ mRNAs (24) and appear to act in a 3′-exonucleolytic degradation pathway (25).

*To whom correspondence should be addressed at: Department of Microbiology, University of Texas at Austin, Austin, TX 78712-1095, USA. Tel: +1 512 475 6350; Fax: +1 512 471 7088; Email: arlen@mail.utexas.edu

[+]Present address: Center for Molecular Medicine and Therapeutics, University of British Columbia, Vancouver, BC V6T 1Z4, Canada

[§]Present address: Ludwig Institute for Cancer Research, University of California San Diego School of Medicine, La Jolla, CA 92093-0660, USA

Table 1. Strains used in this study

Strain number	genotype	plasmid	source
AJY458	*MATa ade2 ade3 leu2 lys2-801 ura3-52 xrn1Δ ski2-14*	pAJ76	this study
BJ5464	*MATα ura3-52 trp1 leu2Δ1 his3Δ200 pep4::HIS3 prb1Δ1.6R can1*		(29)
RDKY1806	*MATα ura3-52 trp1 leu2Δ1 his3Δ200 pep4::HIS3 prb1Δ1.6R can1 xrn1Δ*		this study
CH1305	*MATa ade2 ade3 leu2 lys2-801 ura3-52*		(27)
RDKY1977	*MATa ade2 ade3 leu2 lys2-801 ura3-52 xrn1Δ*		(23)

Table 2. Plasmids used in this study

Plasmid	Relevant markers	Source
pRDK226	Bluescript SKII+ *xrn1::LEU2*	this study
pRDK240	pUC18 *XRN1*	this study
pRDK242	2 micron *URA3 XRN1*	(29)
pRDK246	pUC18 *XRN1*	this study
pRDK249	2 micron *URA3 GAL10::XRN1*	(29)
pRDK252	CEN *URA3 XRN1*	(28)
pRDK287	pUC18 *xrn1Δ2-397*	this study
pRDK288	pUC18 *xrn1Δ2-1076*	this study
pRDK304	2 micron *LEU2 GAL::XRN1(HA)*	this study
pRDK305	CEN *LEU2 XRN1(HA)*	this study
pRDK306	2 micron *LEU2 GAL::XRN1*	this study
pRDK307	CEN *LEU2 XRN1*	this study
pRDK316	2 micron *URA3 GAL10::XRN1*	this study
pRDK317	2 micron *URA3 GAL10*	this study
pRDK318	2 micron *URA3 XRN1(HA)*	this study
pAJ76	2 micron *URA3 ADE3 SKI2*	(17)
pAJ83	CEN *LEU2*	this study
pAJ95	2 micron *LEU2 GAL10::XRN1(HA-HIS6)*	this study
pAJ152	CEN *LEU2 XRN1*	this study
pAJ251	2 micron *LEU2 GAL10::XRN1(HA-HIS6)*	this study
pRIPGKH2(3)Δ1IN1	*URA3 mini-PGK1*	(30)

Xrn1p is the founding member of a class of eukaryotic exoribonucleases that have no significant homology to other known phosphoryl transfer enzymes. In addition, Xrn1p is a nucleic acid binding protein, but again contains no recognizable binding motifs. We sought to carry out a mutational analysis of *XRN1* to identify mutations that affect specific biochemical functions of Xrn1p, in order to correlate characterized *in vitro* functions with different *in vivo* activities. In addition, this analysis would identify residues critical for these functions and begin to define new protein motifs. This analysis consisted of a deletion analysis in which different regions of the gene were deleted and a genetic screen for non-complementing missense mutations. The mutant screen was carried out in an *xrn1 ski2* double mutant which provided a tight genetic background to facilitate the identification of mutants.

MATERIALS AND METHODS

Strains and media

Strains are listed in Table 1. All transformations in *Escherichia coli* were done using DH5α. Rich yeast extract/peptone/dextrose (YPD) and synthetic complete medium lacking uracil (SCUra$^-$) or lacking leucine (SCLeu$^-$) and genetic methods were as described (26). Low adenine plates were as described elsewhere (27). Benomyl sensitivity was assayed as previously described (17). Benomyl was a gift from DuPont Co. and 5-fluoroorotic acid was purchased from US Biological (Swampscott, MA).

Plasmids

Plasmids used in this work are listed in Table 2.

XRN1 C-terminal deletions in 2μ galactose-inducible vectors. To create pRDK316 the oligonucleotide 5′-AGCTTAAGTAGCTAGCGACGT, containing stop codons in all three reading frames, and its complementary oligonucleotide were ligated into the *Aat*II and *Hin*dIII sites of pRDK249. A series of nested C-terminal deletions of *XRN1* in pUC118 (kindly provided by P.Ljungdahl) was digested with *Hin*dIII and *Sst*I and the *XRN1* mutant-bearing fragments were ligated into *Hin*dIII and *Sst*I-digested pRDK316. pRDK317 was derived from pRDK316 by replacing the *XRN1*-containing *Xho*I–*Hin*dIII fragment with oligonucleotide 5′-TCGAGACACCATGGCCACGTGA and its complementary oligonucleotide.

XRN1 C-terminal deletions in CEN vectors. The oligonucleotide 5′-TCGATTCTAGACCCGGGAAGCTTAAGTAGCTAGCT, containing restriction sites for *Xba*I and *Hin*dIII as well as stop codons in each reading frame, was annealed to a complementary

oligonucleotide and ligated into the *Xho*I and *Sst*I sites of pRS315, thereby replacing the polylinker of pRS315 and destroying the *Xho*I and *Sst*1 sites to give pAJ83. To create pRDK307 the *Xba*I–*Hin*dIII *XRN1*-containing fragment from pRDK252 (28) was ligated into the *Xba*I and *Hin*dIII sites of pAJ83. The pUC118-based *XRN1* C-terminal deletion plasmids (above) were digested with *Hin*dIII and *Sst*I and ligated into pRDK307, replacing the wild-type *XRN1* gene.

N-Terminal deletions of XRN1. The *Xba*I–*Hin*dIII fragment containing *XRN1* from pRDK252 was ligated into *Xba*I and *Hin*dIII-digested pUC18 to give pRDK240. Sequences upstream of the *XRN1* translation start in pRDK240 were replaced to give pRDK246 as follows. The oligonucleotide 5′-CGCGGATCCTC-GAGACACCATGGGTATTCCAAAATTTTTCAGG, complementary to the template strand and introducing *Bam*HI, *Xho*I and *Nco*I sites at –16, –11 and –2 respectively, and the oligonucleotide 5′-AAATCATCCAAAATACG, complementary to the non-template strand of *XRN1* at nt 826–842, were used as PCR primers to amplify the 5′-end of *XRN1*. The resulting product was digested with *Bam*HI and *Sst*I and ligated into the respective sites of pRDK240 to give pRDK246. pRDK287, containing the Δ2–397 deletion, removed the 5′-end of *XRN1* coding sequence from nt 3 to 1190. pRDK246 was digested with *Nco*I and *Hin*dIII. The *Nco*I site at –2 was partially filled in with CAT and blunt-ended with S1 nuclease. The *Nco*I site at nt 1182 was blunt-ended with S1 nuclease. The appropriate restriction fragments were ligated together to give the junction sequence 5′-CCATGTTGATG (the start codon is underlined). pRDK288, containing the Δ2–1076 deletion, removed the 5′-end of the *XRN1* coding sequence from nt 4 to 1593. pRDK246 was digested with *Nco*I or *Bgl*II. The resulting recessed 3′-ends were filled in, the linearized plasmids digested with *Spe*I and the appropriate restriction fragments were ligated together to give the junction sequence 5′-CCATGGATCTT (the start codon is underlined).

*2*μ *LEU2 GAL10 XRN1 (pRDK306)*. The GAL10–*XRN1*-containing *Bam*HI–*Hin*dIII fragment from pRDK249 (29) was ligated into the corresponding sites in YEp351.

*2*μ *LEU2 GAL10 XRN1-HA (pRDK304)*. *XRN1* contains seven *Eco*RI sites, five of which are in the same reading frame. The oligonucleotide 5′-AATTACCCATACGACGTCCCAGACTA-CGCTAGC, encoding the hemagglutinin (HA) epitope and containing *Aat*II and *Nhe*I restriction sites, and its complementary strand, 5′-AATTGCTAGCGTAGTCTGGGACGTCGTATGGGT, were annealed and ligated into linearized pRDK242 (29) partially digested with *Eco*RI. The ligation mix was transformed into *E.coli* and DNA prepared in batch from all transformants. The batch-prepared DNA was then transformed into RDKY1806 (*xrn1*::*LEU2*). Transformants were screened for HA expression and complementation of the growth defect of *xrn1*Δ. Six isolates were identified and all contained an oligonucleotide insertion in the *Eco*RI site at nt 3894 of *XRN1*, giving pRDK318. HA-*XRN1* containing the *Sst*I–*Hin*dIII fragment of pRDK318 was ligated into the corresponding sites of pRDK306 to give pRDK304.

*2*μ *LEU2 GAL10 XRN1(HA-HIS6) (pAJ95)*. The oligonucleotide 5′-CTAGGCATCATCATCATCATCATA, encoding six histidines, and a complementary oligonucleotide were annealed and ligated into the *Nhe*I site previously introduced into *XRN1* by the HA-containing oligonucleotide in pRDK304. This plasmid expresses Xrn1p containing both HA and 6×HIS. pRDK305 was prepared by replacing the *XRN1*-containing *Sst*I–*Hin*dIII (1336–2239 nt) fragment of pRDK307 with the *XRN1*-HA containing *Sst*I–*Hin*dIII fragment from pRDK318. pAJ152 was prepared by fusion PCR to introduce a unique *Xho*I site at –12 of *XRN1* in pRDK305. The resulting sequence change, TATATCTC-GAGTACGGTATG, (underlining shows altered nucleotides and the start codon), was confirmed by sequencing. pAJ251 was derived from pAJ95 by digestion with *Sap*I and *Hin*dIII, end-filling and re-ligation, thus eliminating an *Sst*I site upstream of *XRN1* in pAJ95. Plasmid pRIPGKH2(3)Δ1IN1, referred to in this work as mini-PGK1 (30), was a gift from S.Peltz.

Genetic methods

The *XRN1* coding sequence from nt 108 to 3894 was replaced by the *LEU2* gene to give the pUC18-based plasmid pRDK226. pRDK226 was digested with *Hin*dIII and *Avr*II and transformed into BJ5464 to generate the *xrn1*::*LEU2* allele. Correct integrants were identified by PCR to give RKY1806.

Overexpression of truncated Xrn1 proteins

Overnight cultures grown at 30°C in SCUra$^-$ medium supplemented with 2% raffinose were diluted in the same medium to 1.5×10^7 cells/ml and galactose was added to 2%. The cultures were incubated at 30°C for 4–5 h and the cells harvested. Small scale extracts were prepared as described previously (29). Western blotting was performed as described (16), using affinity-purified polyclonal anti-Xrn1p (16) or monoclonal 12CA5 anti-HA (Berkeley Antibody Co.).

Northern blot analysis and nucleic acid substrates

Total yeast RNA was prepared and analyzed by northern blotting for ITS1 and CYH2 as described previously (17). Additional oligonucleotide probes were specific for the pre-CYH2 intron (5′-CTGGACATTTTATCGAAACAAAAGAAACGTGG) and for mini-PGK1 (5′-CGATAGTAATATTTATATATTTATATTTTT-AAAATATTTA). The substrate for *in vitro* exoribonuclease assays, corresponding to the 5′ 261 nt of pre-CYH2 mRNA, was prepared by *in vitro* transcription using a T7 Ribomax kit (Promega) in the presence of [α-^{32}P]CTP. Specific activity of the substrate was typically 80–100 c.p.m./pmol nucleotide. The template was prepared by PCR of the endogenous yeast *CHY2* gene using the primers 5′-CGCGGATCCTAATACGACTCACTA-TAGAACAATCATCCAACTAATC, containing the T7 promoter and transcription start site for *CYH2*, and 5′-AAGCCGTCTCAAC-AGTGAGATGGTA. The 5′-triphosphate was hydrolyzed to 5′-monophosphate using tobacco acid pyrophosphatase (Epicentre) as described elsewhere (11) and the RNA was purified by phenol extraction and ethanol precipitation. T7 [^{3}H]DNA was prepared as described previously (31).

Single-strand DNA exonuclease assay

Reactions contained 33 mM Tris, pH 8.5, 13 mM $MgCl_2$, 88 μg/ml BSA, 1.8 mM dithiothreitol, heat-denatured T7 [^{3}H]DNA (22 000 c.p.m.) and crude cell extract (0.1–1 μl) in a 30 μl volume. After incubation at 30°C for 20 min, the reactions were stopped on ice by addition of 10 μl 20 mM EDTA containing 1 mg/ml heat-denatured calf thymus DNA followed by 40 μl 1 M trichloroacetic acid. The mixture was incubated on ice for 10 min and centrifuged for 10 min and 60 μl supernatant were analyzed

by liquid scintillation counting. Net activity was determined by subtracting the activity measured in a mock reaction. The limit of detection in this assay was 10% of wild-type activity.

Screen for non-complementing *xrn1* missense mutations

PCR was used to generate mutations in four contiguous regions of *XRN1*. PCR reactions contained 100 ng plasmid template DNA, 10 pmol each primer, 5 mM $MgCl_2$, 0.2 mM nucleotides and 2 U Taq DNA polymerase (Promega) in a 50 µl volume. Denaturation at 94°C for 2.5 min was followed by 12 cycles of 0.5 min denaturation at 94°C, 1 min annealing at 45°C and 1 min extension at 72°C per 1 kb DNA. Ten independent PCR reactions were carried out simultaneously and were combined after PCR was complete. Region I, nominally from nt 1 to 293 of *XRN1*, was amplified with primers 3196 (5′-TTGGGATTTTAAATGCC) and 3205 (5′-AGTTTATTTTCTAAAGG) using pAJ152 as the template. The resulting PCR product (corresponding to nt –151 to 573) was co-transformed with pAJ152 digested with *Xho*I (nt –12) and *Sst*I (nt 293) into AJY458 and plated on SCLeu⁻ low Ade plates. Region II, from nt 293 to 1335, was amplified similarly using primers 2462 (5′-GAACACAGATTCCTGAG) and 2463 (5′-CCAATTCTTTTTGTCC). The resulting PCR product was digested with *Sst*I and *Bsm*I, ligated into *Sst*I and *Bsm*I-digested pAJ152 and transformed into *E.coli*. A DNA library was prepared from the combined transformants and the library DNA was transformed into AJY458 and plated on SCLeu⁻ low Ade plates. Region III, nt 1335–2239, was amplified similarly, using PCR primers 3213 (5′-CAGGAAAAATTATCGCC) and 2836 (5′-TTTAAATGCCTCTTGG). The resulting product was digested with *Bsm*I and *Spe*I and ligated into *Bsm*I and *Spe*I-digested pAJ152. Region IV, nominally from nt 2239 to 3612, was amplified with primers 3216 (5′-ACACAATCATTGTGTCG) and 3254 (5′-GAAAGAGGCATCAAGCC). The PCR product was co-transformed with pAJ152 digested with *Spe*I (nt 2239) and *Bcl*I (nt 3612) into AJY458. Non-complementing *XRN1* mutants were identified as non-sectoring colonies and arose at a frequency of ~2% for region I and 4% for regions II, III and IV. To eliminate nonsense mutants, 50 region I mutants, 173 region II mutants, 109 region III mutants and 96 region IV mutants were screened by western blotting for expression of Xrn1p containing the HA epitope located in the C-terminus of the protein. This yielded 10 missense mutations in region I, six in region II, one in region III and one in region IV. Region I and II mutants containing multiple mutations were sub-cloned to identify single amino acid changes responsible for the non-complementing phenotype. The region III and IV mutants each contained multiple changes and were analyzed without sub-cloning. All mutant *xrn1* genes were sub-cloned to a galactose-inducible expression vector to facilitate affinity purification for *in vitro* analysis.

Immunoprecipitation of epitope-tagged Xrn1p

Cell cultures of BJ5464 bearing 2µ plasmids with galactose-inducible *xrn1* mutants were grown in 25 ml SCLeu⁻ containing 2% raffinose to a density of 1.5×10^7 cells/ml. For controls, cultures of BJ5464 containing wild-type HA-tagged *XRN1* on pAJ251 or the empty vector, YEp351, were prepared. Galactose was added to 2% final concentration and the cells were incubated for 6 h before harvesting and storage at –80°C. Small scale extracts were prepared by glass bead disruption in 500 µl 20 mM Tris–HCl, pH 7.5, 150 mM NaCl, 1 mM EDTA, 1 mM DTT and 1 mM PMSF. The extracts were clarified by centrifugation at 15 000 *g* for 10 min at 4°C. For immunoprecipitation, 100 µg total protein (typically 10 µl extract) were diluted into 500 µl IP buffer (20 mM Tris, pH 7.5, 500 mM NaCl, 1% NP40, 0.1 mg/ml BSA, 1 mM EDTA, 1 mM PMSF, 1 µM pepstatin A and 1 µM leupeptin) on ice. A limiting amount of 12CA5 antibody (0.03–1 µg) was added and the samples were incubated on ice for 1 h. Subsequently, 15 µl of a slurry of protein A–agarose beads (Gibco) was added and the samples rocked gently at 4°C for 30 min. The beads were centrifuged, washed three times with 250 µl IP buffer and assayed immediately. Western blotting showed that under these conditions the amount of Xrn1p immunoprecipitated was proportional to the amount of 12CA5 antibody added (data not shown).

Exoribonuclease assay of immunoprecipitated wild-type and mutant Xrn1p

The protein A beads containing the bound Xrn1p–antibody complex were washed once in exonuclease buffer (20 mM Tris, pH 8.5, 75 mM NaCl, 5 mM $MgCl_2$, 0.1 mg/ml BSA, 0.2 mM DTT) and the beads were resuspended in 30 µl reaction mix, 20 mM Tris–HCl, pH 8.5, 75 mM $NaCl_2$, 5 mM $MgCl_2$, 0.1 mM BSA, 0.2 mM DTT and 5000 c.p.m. [^{32}P]pre-CYH2 RNA. Reactions were incubated for 10 min at 30°C and then stopped on ice with addition of 10 µl 1 mg/ml single-stranded DNA, 20 mM EDTA and 66 µl 0.6 M trichloroacetic acid. After 10 min on ice, the samples were centrifuged for 10 min at 4°C and 80 µl of the supernatant were removed for liquid scintillation counting. Net activity was determined by subtracting the activity measured in a mock reaction, containing an immunoprecipitate from an extract lacking HA-tagged Xrn1p. Activities were normalized to the amount of Xrn1p that was immunoprecipitated.

RESULTS

Sequence alignment of Xrn1p with related proteins suggests that the protein is composed of distinct domains (Fig. 1). The N-terminus, conserved among all family members, is acidic and contains two highly conserved regions. Previous work demonstrated a V8 protease-sensitive site at amino acid 501 (28), suggesting that the two conserved acidic blocks are separate domains. Since only these acidic domains are found in both the Rat1p and Xrn1p sub-families, they likely contain the exonuclease (see below). A middle basic domain is common to the Xrn1p sub-family. Protease digestion of Xrn1p under native conditions identified a second V8-sensitive site at amino acid 710, a chymotrypsin-sensitive site at position 723 and a trypsin-sensitive site at position 730 (28), demonstrating accessibility at the boundary of the acidic and basic domains. The basic extreme C-terminus of Xrn1p is unique to this protein and is sensitive to proteolysis. Initial purification of Xrn1p yielded a proteolyzed protein lacking the extreme C-terminus. This truncated protein retained exonuclease activity (29; unpublished data), implying that the C-terminus is a distinct domain dispensable for exonuclease activity.

A series of deletion mutants of *XRN1* was constructed to identify functional domains of Xrn1p. These deletion mutants were expressed from single copy vectors for complementation assays *in vivo* or from high copy vectors under control of the galactose-inducible *GAL10* promoter for *in vitro* analysis. *xrn1* null mutants display a significant growth defect (4). This growth defect was complemented by mutant proteins containing small deletions from the C-terminus, mutants Δ1493–1528 and

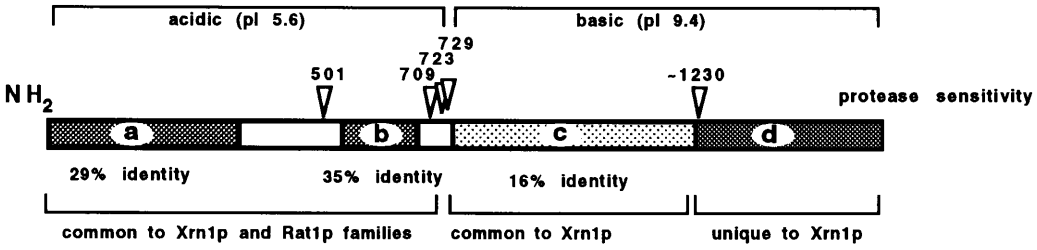

Figure 1. General structure of Xrn1p based on amino acid sequence alignment and protease sensitivity. Conserved domains a, b and c and domain d, unique to Xrn1p, are shaded. Percent identity for domains a and b is the percent of amino residues that are invariant among six proteins: Xrn1p and Rat1p from *S.cerevisiae* (4,37), ExoII and Dhp1 from *S.pombe* (13,18) and mXRN1p and Dhm1 from mouse (14,19). The percent identity for domain c reflects identity only among the Xrn1p sub-family, Xrn1p, Dhp1 and mXRN1p. Open arrowheads indicate sites of protease cleavage under native conditions (28). Numbers indicate the amino acid position C-terminal of cleavage. The cleavage at amino acid 1230 is approximate, based on comparisons of the relative mobilities of the proteolyzed protein and truncation proteins on SDS–polyacrylamide gels.

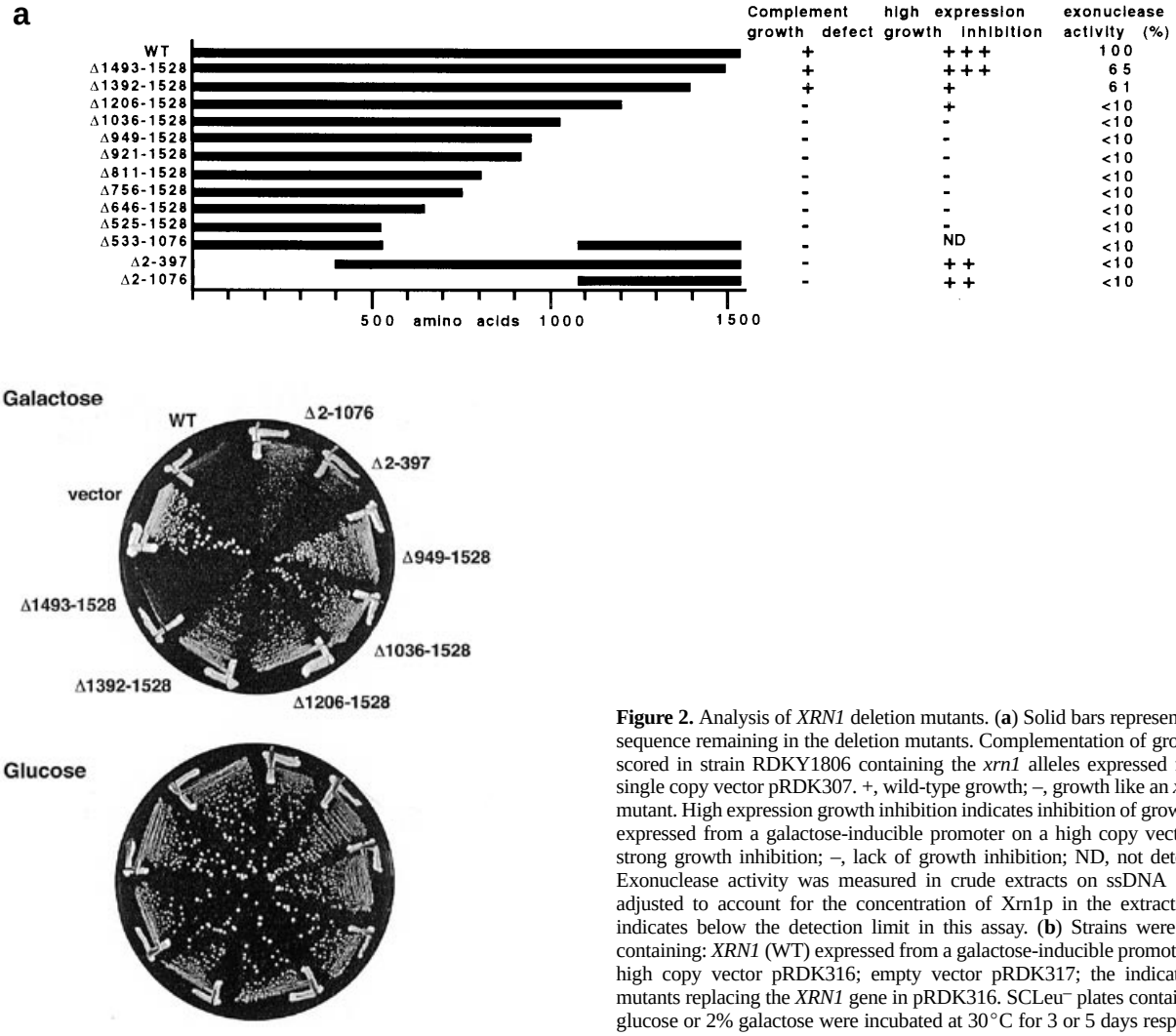

Figure 2. Analysis of *XRN1* deletion mutants. (**a**) Solid bars represent protein sequence remaining in the deletion mutants. Complementation of growth was scored in strain RDKY1806 containing the *xrn1* alleles expressed from the single copy vector pRDK307. +, wild-type growth; –, growth like an *xrn1* null mutant. High expression growth inhibition indicates inhibition of growth when expressed from a galactose-inducible promoter on a high copy vector. +++, strong growth inhibition; –, lack of growth inhibition; ND, not determined. Exonuclease activity was measured in crude extracts on ssDNA and was adjusted to account for the concentration of Xrn1p in the extracts. <10% indicates below the detection limit in this assay. (**b**) Strains were BJ5464 containing: *XRN1* (WT) expressed from a galactose-inducible promoter on the high copy vector pRDK316; empty vector pRDK317; the indicated *xrn1* mutants replacing the *XRN1* gene in pRDK316. SCLeu$^-$ plates containing 2% glucose or 2% galactose were incubated at 30°C for 3 or 5 days respectively.

Δ1392–1528, but not by mutant proteins containing larger deletions from the C-terminus nor by proteins containing deletions of the N-terminus or internal sequences of the protein (Fig. 2 and data not shown). Consistent with this result, the two mutants Δ1493–1528 and Δ1392–1528 were also the only mutant proteins tested that complemented the inviability of an *xrn1 ski2* double mutant (data not shown). All mutant proteins were present at similar high levels in total protein extracts (data not shown), suggesting that the lack of complementation was not a consequence of altered expression or protein stability.

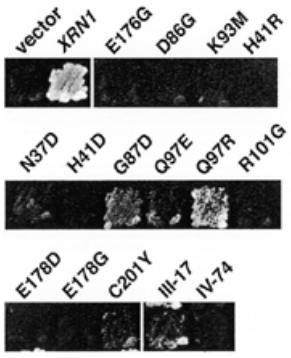

Figure 3. Assay for complementation of *xrn1 ski2* by *xrn1* mutants. Strain AJY458, which contains *SKI2* on a *URA3* vector, was transformed with single copy vectors containing the *xrn1* point mutants. Transformants were patched to a plate containing 5-fluoroorotic acid. Growth on this plate requires loss of the *SKI2 URA3* plasmid and indicates complementation of *xrn1 ski2*.

The extreme C-terminus of Xrn1p confers a dominant negative phenotype

Full-length wild-type Xrn1p inhibited cell growth when over-expressed from a high copy plasmid under the control of a galactose-inducible promoter (Fig. 2b). The *xrn1* deletion mutants were tested for this growth inhibition phenotype. Overexpression of the mutant Δ1493–1528, lacking only the C-terminal 36 amino acids, conferred strong growth inhibition similar to the wild-type. Slightly larger deletions, Δ1392–1528, which retains a functional exonuclease, and Δ1206–1528, which lacks exonuclease activity, displayed modest growth inhibition. Larger deletions from the C-terminus restored growth similar to that of cells containing the empty vector, indicating a lack of growth inhibition (Fig. 2b and data not shown). The N-terminal deletions Δ2–397 and Δ1–1076 showed moderate growth inhibition, intermediate between that observed for the wild-type and mutant Δ1392–1528. These results indicate that the C-terminal domain that is unique to Xrn1p confers dominant negative growth inhibition when overexpressed. This activity is primarily located within amino acids 1392–1492, although amino acids from 1036 to 1391 contribute a modest level of growth inhibition. The conserved N-terminus of Xrn1p, which likely contains the exonuclease, is not necessary for the growth inhibition phenotype. Thus, these data suggest that growth inhibition is independent of nuclease function (see below).

The *xrn1* deletion mutant proteins were overexpressed and assayed *in vitro* for exonuclease activity. We took advantage of the fact that Xrn1p demonstrates exonuclease activity on single-stranded DNA as well as RNA to avoid contaminating exoribonucleases in the crude extracts. Consistent with the *in vivo* complementation results, C-terminal deletions up to amino acid 1392 displayed high levels of exonuclease (60% of wild-type; Fig. 2), whereas larger deletions lacked detectable activity.

Non-complementing missense mutations in *XRN1*

The deletion mutant analysis did not reveal the location of the exonuclease domain of Xrn1p. Consequently, point mutations were generated and screened for non-complementing missense mutations (see Materials and Methods). PCR was used to make random mutations within four contiguous regions of the gene corresponding to amino acids 1–1203. Nineteen non-complementing *xrn1* missense mutants were identified based on their inability to complement an *xrn1 ski2* double mutant. Seventeen of the mutants were within regions I (nt 1–293) and II (nt 294–1335). Of these, seven contained two nucleotide changes and one contained three nucleotide changes. Only two of the mutants containing multiple nucleotide changes resulted in second amino acid changes, E176G F29L and E178G Q401L. These two mutants were sub-cloned to separate the mutations. The single mutations E176G and E178G both conferred a null phenotype, whereas F29L and Q401L showed no obvious phenotype. Of the 17 region I and II mutants, three were represented twice, giving 14 different single amino acid changes of highly conserved residues mapping from amino acid 37 to 201 (Figs 3 and 4 and Table 3). Two additional mutants, referred to as III-17, from region III (nt 1336–2239), and IV-74, from region IV (nt 2240–3612), contained multiple amino acid changes between amino acids 592 and1197 and these mutants were analyzed without sub-cloning. Mutant Q97R showed a low level of complementation of *xrn1 ski2* (Fig 3), consistent with having the highest level of exoribonuclease activity among the mutants (Table 3). Mutant G87D showed very weak complementation (Fig. 3) but no measurable exonuclease activity *in vivo* (Figs 5 and 6) or *in vitro* (Table 3). Further characterization of this mutant is required to understand how it provides complementing activity. It is possible that the mutant protein acts by efficiently sequestering substrates without degradation. When the *xrn1* point mutants were tested for their ability to complement the synthetic lethality of *xrn1 ski3* double mutants, results similar to those shown in Figure 3 were obtained (data not shown), suggesting that the exonuclease function of Xrn1p is required in *ski3* mutants as well.

Table 3.

amino acid change	number of isolates	relative net RNase activity[a]	relative net DNase activity[a]
N37D	1	0.03	<10
H41R	1	0.03	20
H41D	1	<0.01	<10
D86G	1	0.02	<10
K93M	1	<0.01	<10
G87D	1	<0.01	<10
Q97E	1	0.04	14
Q97R	1	0.61	11
R101G	1	0.03	<10
E176G	2	<0.01	<10
E178D	2	0.16	12
E178G	2	<0.01	<10
C201Y	1	ND	ND
C201R	1	0.03	<10
III-17 (L592P,Y710C)	1	<0.01	<10
IV-74 (W798R,E1024D, Y1043F,S1197P)	1	<0.01	<10

[a]Activity is expressed relative to that of wild-type HA-tagged Xrn1p, after correcting for activity in reactions lacking HA-tagged Xrn1p.

Northern blot analysis of *xrn1* mutants

Northern blotting was done on total RNA isolated from *xrn1* mutant strains containing the *xrn1* point mutants expressed from single copy vectors. Blots were probed for ITS1, CYH2 and mini-PGK1. ITS1 is a product of rRNA processing that is rapidly degraded in wild-type cells by Xrn1p (8). As seen in Figure 5, all of the mutants tested displayed stabilization of ITS1 *in vivo*,

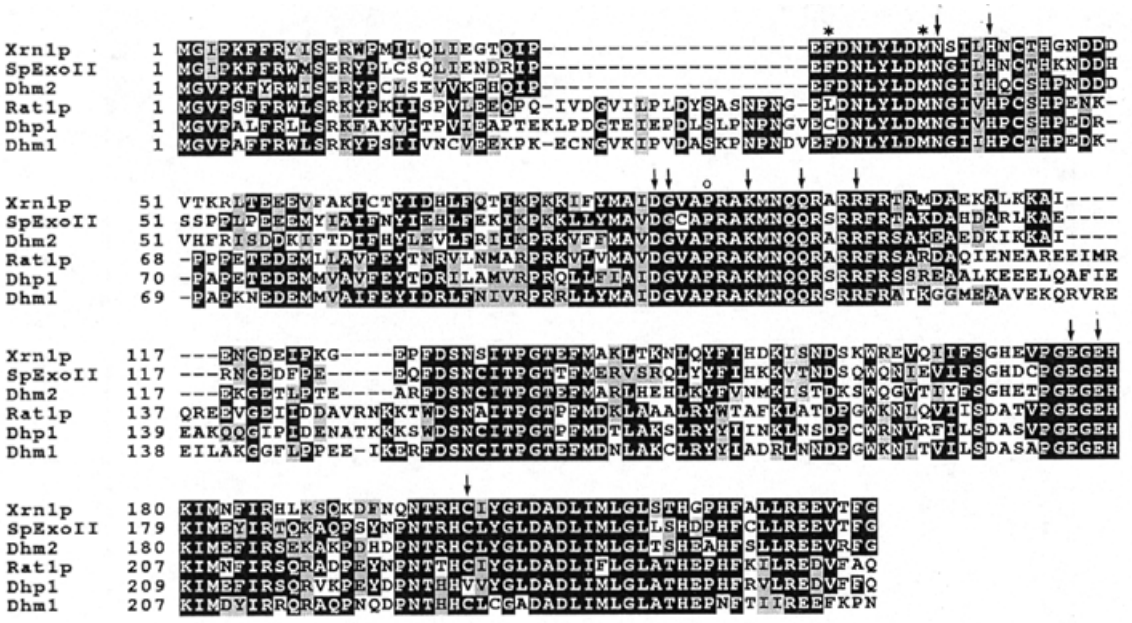

Figure 4. Homology alignment and positions of amino acid changes identified in *xrn1* mutants. The top three lines of alignment are the Xrn1p sub-family: ExoII, from *S.pombe*; Dhm2, from mouse. The lower three lines are the Rat1p sub-family: Dhp1, from *S.pombe*; Dhm1 from mouse. Arrows indicate residues affecting exonuclease activity that were altered in *xrn1* point mutants. Asterisks represent residues that could be changed in Xrn1p (F29L) or Rat1p (M36T) without affecting nuclease activity. The open circle indicates the position of the amino acid change (P90L) in the *xrn1-10*^{ts} allele.

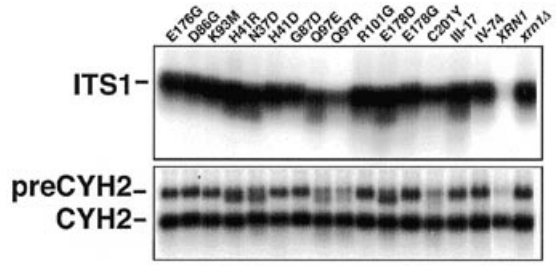

Figure 5. Northern blot analysis of *in vivo* substrates of Xrn1p. Ten micrograms of total RNA were separated on a 1.2% agarose–formaldehyde gel, transferred to nylon membrane and probed with a probe specific for ITS1 or CYH2. Strains were RDKY1977 containing the indicated *xrn1* alleles in the single copy vector pAJ152 and were grown in SCLeu$^-$. III-17 and IV-74 contain multiple amino acid changes (see Table 3).

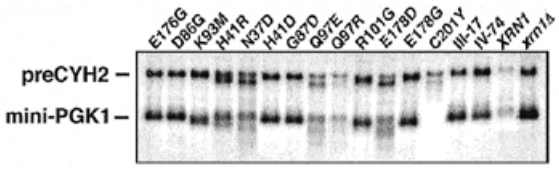

Figure 6. Northern blot analysis of nonsense codon-containing mRNAs. Conditions were as described in Figure 5 except that the strains used here also contained the mini-PGK1 allele on pRIPGKH2(3)Δ1IN1 (30) and strains were grown in SCLeu$^-$Ura$^-$. The blot was probed simultaneously with an intron-specific probe for pre-CYH2 and with a probe specific for mini-PGK1.

indicating that all were defective for exonuclease activity. The degree of stabilization and the nature of the ITS1 signal varied among the mutants. Whereas most mutants stabilized intact ITS1, some of the mutants, e.g. Q97E and E178D, showed broadening of the ITS1 band to lower molecular weight, suggesting partial degradation.

Analysis of pre-CYH2 RNA also demonstrated defects in *in vivo* degradation, but in addition revealed novel degradation intermediates. CYH2 pre-mRNA is inefficiently spliced in yeast and the pre-mRNA is rapidly degraded in the cytoplasm by Xrn1p after decapping by the deadenylation-independent nonsense-mediated decay pathway (3). Again, varying degrees of stabilization of pre-CYH2 were observed. However, some of the mutants, notably N37D, H41R, Q97E, Q97R and E178D, gave rise to new bands corresponding to CYH2 pre-mRNA ~100 nt shorter than full length. These new species represented RNAs that had been only partially degraded from the 5′-ends and were not due to altered processing from the 3′-end, since they contained poly(A) tails which could be removed by RNase H digestion in the presence of oligo(dT) without altering the relative position of the pre-CYH2 to the degradation intermediates (data not shown). Pre-CYH2 RNA was also analyzed with an intron-specific probe (Fig. 6). Simultaneously, these RNAs were probed with a mini-PGK1-specific probe. Both of these RNAs are degraded by nonsense-mediated decay. In both cases, discrete degradation intermediates were observed. Interestingly, amino acid substitution of H41 and E178 gave rise to different phenotypes dependent on the amino acid substitution. Conservative changes that maintained charge (H41R and E178D) resulted in mutants that showed degradation intermediates, whereas the non-conservative changes H41D and E178G resulted in a complete blockage of degradation, indicated by stabilization of the full-length RNAs.

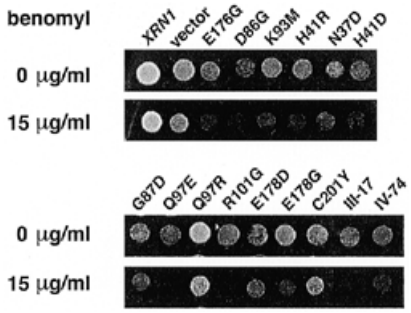

Figure 7. Benomyl hypersensitivity of *xrn1* exonuclease mutants. Cultures of strain RDKY1977, containing the indicated *xrn1* alleles on the single copy vector pAJ152, were spotted onto YPD plates containing 0 or 15 μg/ml benomyl. Plates were incubated at 30°C for 2 days.

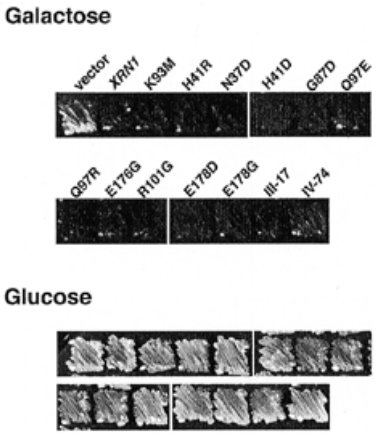

Figure 8. Growth inhibition from overexpression of *XRN1* does not require exonuclease activity. Cultures of strain BJ5464, containing the indicated *xrn1* alleles under control of a galactose-inducible promoter on the high copy plasmid pAJ251, were patched onto SCLeu⁻ plates containing 2% glucose or 2% galactose and incubated at 30°C for 3 days.

Some transcript-specific differences were observed. For example, mutant C201Y displayed wild-type degradation of mini-PGK1 mRNA but accumulated degradation intermediates of CYH2 pre-mRNA.

The degradation intermediates resulted from mutant Xrn1p processing, since they were not seen in the absence of Xrn1p (Figs 5b and 6). Also, accumulation of these intermediates was not observed when the mutant protein N37D or E178D was overexpressed in a wild-type strain, indicating that wild-type Xrn1p can degrade these RNAs in the presence of mutant Xrn1p (data not shown). This suggests that the mutant proteins do not remain tightly bound to the substrate, impeding degradation by wild-type protein. Taken together, the novel degradation intermediates appear to result from mutant Xrn1p being blocked either by proteins bound to the transcript or by secondary structure in the transcript.

In vitro exonuclease activities

The mutant and wild-type Xrn1p proteins were overexpressed and purified from crude extracts of wild-type yeast by immunoprecipitation, taking advantage of the HA epitope in their C-terminus. All mutant and wild-type proteins were expressed at similar levels, suggesting that all proteins had similar stability. The immunoprecipitated proteins were then assayed for exoribonuclease activity without further purification. For these assays, the substrate was an *in vitro* synthesized transcript corresponding to the first 261 nt of the 5′-end of CYH2 pre-mRNA. Xrn1p concentration in the assays was controlled by titrating the Xrn1p proteins with limiting amounts of anti-HA antibody. Under these conditions, the amount of Xrn1p in the assays was proportional to the amount of anti-HA used for immunoprecipitation (data not shown). Results of these assays are shown in Table 3. The *in vitro* activity closely paralleled the *in vivo* activity observed on ITS1, pre-CYH2 and mini-PGK1. These assays were remarkably free of contaminating exoribonucleases and the level of detection was <2% of wild-type Xrn1p activity.

The mutant proteins were also assayed for single-strand DNA exonuclease activity. This assay was done with crude extracts without immunopurification. Under these conditions, overexpressed Xrn1p accounts for ~90% of the total exonuclease activity in these extracts. As seen in Table 3, all mutant proteins displayed reduced DNA exonuclease activity that in general corresponded to the decrease in exoribonuclease activity, suggesting that these activities reside in the same active site. One exception, Q97R, displayed much lower relative DNase activity compared with RNase activity. It is not clear at present what accounts for this difference, but it may be due to differences in binding deoxyribose compared with ribose. The correlation of RNase and DNase activities suggests that these activities are both manifest by the same active site.

xrn1 nuclease-deficient mutants do not complement the benomyl-hypersensitive phenotype of *xrn1* null mutants

Benomyl destabilizes microtubules and mutants that display microtubule defects often confer hypersensitivity to benomyl (32). Such hypersensitivity of *xrn1* mutants has led to the suggestion that Xrn1p may interact directly with tubulin (22). We tested the various *xrn1* point mutants for their ability to complement the benomyl sensitivity of an *xrn1* null mutant. There was a general correlation between the severity of the exonuclease defect and inability to complement benomyl hypersensitivity. Mutants that lacked detectable exonuclease activity, e.g. E178G and H41D, were at least as sensitive as an *xrn1* null mutant, whereas Q97R, which displayed 60% of wild-type exonuclease activity and partially restored growth to an *xrn1 ski2* double mutant, partially restored wild-type sensitivity to benomyl (Fig. 7).

Growth inhibition from overexpression of Xrn1p does not depend on exonuclease

The dominant negative phenotype that results from overexpression of the C-terminus of Xrn1p was also observed for all of the missense mutants (Fig. 8). Thus, growth inhibition is not due to overexpression of the nuclease activity of Xrn1p, but rather some other as yet unidentified function of the protein.

DISCUSSION

Xrn1p is the founding member of a family of eukaryotic exoribonucleases. It is the major activity in the cytoplasm of yeast responsible for mRNA degradation and is also responsible for the elimination of rRNA processing fragments and improperly processed mRNAs subject to nonsense-mediated decay. In yeast,

a second but essential 5′-exoribonuclease, encoded by *RAT1*, is found in the nucleus (17). These two enzymes are functionally interchangeable, although normally restricted to the cytoplasm and nucleus respectively (17). Homologs of Xrn1p and Rat1p have been identified from higher eukaryotes, including *D.melanogaster* (D.Till, B.Linz, J.Seago, J.McClellan, J.McCarthy and S.F.Newbury, personal communication) and mouse (14,19), however, no homologs of these proteins have been identified from prokaryotic cells.

Xrn1p and its homologs are large proteins that contain exonuclease as well as nucleic acid binding activities, although they share no obvious sequence motifs with other classes of proteins. In addition, Xrn1p has been implicated in additional cellular processes, including interaction with tubulin (22). Thus, it is of interest to identify the structural motifs of these proteins responsible for their biochemical properties and to identify mutations within these motifs that eliminate specific biochemical functions to correlate these functions with observed phenotypes.

This family of proteins can be aligned based on primary amino acid sequence, revealing an acidic N-terminal half of the protein composed of two domains of striking homology common to all family members (Fig. 1). Since this acidic region of the protein is the only portion common to this family of exonucleases, it likely contains the exonuclease. C-terminal to this, the Xrn1p and Rat1p sub-families diverge in amino acid sequence. However, the sub-families each contain basic domains and thus may have conservation at a gross structural level. The extreme C-terminus of Xrn1p, again basic, is unique to this protein. The apparent arrangement of these proteins into domains based on sequence alignments is reflected in the susceptibility of Xrn1p to proteolysis under native conditions. Protease cleavage of Xrn1p for amino acid sequencing using several different proteases yielded cleavage at amino acid 501, between the two blocks of amino acid conservation within the N-terminal acid half of the protein and after amino acids 710, 723 and 730, suggesting that the boundary between the highly conserved acidic N-terminus and the following basic domain is readily accessible to proteases (28). In addition, the extreme C-terminus, unique to Xrn1p, is highly susceptible to proteolysis during purification (29).

Surprisingly, although the protein appears to be a linear assemblage of domains, deletion of any portion of the homologous domains rendered the protein completely inactive *in vivo* and *in vitro*, even though subsequent point mutation analysis suggested that the N-terminus contains the exonuclease. Thus, this analysis failed to localize the exonuclease domain of the protein. We do not yet understand why this protein is not amenable to deletions, but it may reflect changes in the overall net charge of the protein when portions of an acidic or basic domain are deleted.

Deletions of the extreme C-terminus do not affect most *in vivo* functions, but the C-terminus does confer growth inhibition when the protein is overexpressed. This growth inhibition depended primarily on amino acids 1392–1492 and was observed for constructs containing large N-terminal deletions. However, high expression growth inhibition was observed for exonuclease-deficient point mutants, demonstrating that it was not due to the overexpression of the exonuclease activity. It is possible that the C-terminus interacts with other essential cellular components, titrating them to below critical levels. Two-hybrid analysis with the C-terminal domain should identify such factors.

Point mutations identify residues critical for exonuclease function

The screen employed for identifying point mutants required that such mutants not complement an *xrn1 ski2* double mutant. All *xrn1* mutations identified in this screen reduced or abolished detectable exonuclease activity, suggesting that synthetic lethality with a *ski2* mutation (23) is due specifically to a lack of Xrn1p exonuclease activity. This was not a foregone conclusion. Xrn1p is also an RNA binding protein and defects in RNA binding could conceivably be lethal in combination with a *ski2* mutation. In addition, Ski2p suppresses translation of poly(A)$^-$ mRNA (24,33). Ski2p may be necessary to confer specificity of ribosomes for poly(A) mRNA or by acting in a degradation pathway that degrades such mRNA. The requirement for nuclease activity for complementation of a *ski2* mutation is consistent with the finding that *SKI2* is necessary for a 3′ mRNA degradation pathway (25). In this model, residual 3′ degradation controlled by Ski2p is essential in the absence of the major 5′ degradation pathway, which requires Xrn1p. This screen did not identify mutations in other regions of the protein or shed light on other functions of Xrn1p. To identify other functions of Xrn1p, we are currently screening additional mutants that are synthetically lethal with an *xrn1* null mutant for complementation by an *xrn1* exonuclease-deficient mutant.

The Xrn1p family of proteins does not contain amino acid sequences that are readily identifiable as exonuclease or RNA binding motifs. However, all single point mutants identified in this screen reduced or abolished detectable nuclease activity and were localized to the highly conserved N-terminal domain of Xrn1p. At least some of these residues are likely within the active site of the exonuclease. Like many nucleases, Xrn1p requires Mg^{2+} for activity. Structural and biochemical studies of other nucleases have shown that such divalent cations are typically coordinated by carboxylates (34–36). In Xrn1p, several invariant carboxylate residues, D86, E176 and E178, appeared to be essential for function. Replacement of E178 with aspartate, a conservative change that maintains a carboxylate moiety, reduced the nuclease activity but did not eliminate it, whereas the more drastic change to a glycine eliminated detectable activity altogether. Possibly E178 coordinates a metal ion and replacing E178 with aspartate leads to a less favorable coordination. Similarly, H41 is important for nuclease function. Changing H41 to arginine maintains the charge and results in a protein with reduced activity, whereas the more drastic change to aspartate eliminates detectable activity.

During the course of this work, the *xrn1-10* temperature-sensitive mutation (23) was identified as P90L. This mutation disrupts exonuclease activity at non-permissive temperature (A.Johnson, unpublished results) and lies within a highly conserved block of amino acids. In addition, changing F29 in Xrn1p or changing M36 in Rat1p had no significant affect on enzyme activity (A.Johnson, unpublished results). Thus, some changes of highly conserved residues do not significantly affect function, suggesting that the mutations identified in this screen were particularly critical for nuclease activity.

All mutants were defective to varying degrees for exonuclease activity measured *in vivo* by northern blot analysis of several different RNAs and by *in vitro* assays. In general, the *in vivo*

activities correlated with the *in vitro* activities. In addition, there was a good correlation between the amount of residual exonuclease activity and the ability to complement an *xrn1 ski2* double mutant. Furthermore, mutations that affected the exoribonuclease activity of Xrn1p also affected in a similar fashion its activity on single-stranded DNA, suggesting that these two activities are manifested by the same active site.

An interesting class of *xrn1* mutants yielded novel degradation intermediates on mRNAs targeted for rapid degradation in the deadenylation-independent nonsense-mediated decay pathway. These mutants displayed reduced exonuclease activity measured *in vitro* and were unable to completely degrade certain RNAs *in vivo*. It is possible that these mutants have reduced processivity, although the exact nature of their defect will require more extensive *in vitro* characterization with purified mutant proteins. These mutants are not dominant, suggesting that the novel RNA intermediates are not due to mutant Xrn1p binding tightly to RNA and thereby inhibiting the progress of wild-type Xrn1p. The intermediates most likely are due to blockage by either the intrinsic structure of the RNA or proteins bound to the RNA. We are currently examining the nature of the block on the RNA. Preliminary *in vitro* results suggest that although the mutant proteins have reduced exonuclease activity, they are not blocked at a discrete point on pre-CYH2, suggesting that the degradation block is formed *in vivo* and may be due to proteins on the RNA. Possibly, Xrn1p is responsible for displacing proteins on the transcript, for example ribosomes, as the RNA is degraded.

It has been reported that Xrn1p is a tubulin binding protein based on genetic and *in vitro* studies (22), which concur with the initial report that *xrn1* mutants are hypersensitive to the tubulin destabilizing drug benomyl (4). We tested the *xrn1* point mutants described here for their ability to complement benomyl hypersensitivity. There was a good correlation between the ability to complement and the amount of residual exonuclease activity displayed by the mutant. Mutants with no detectable exonuclease activity were unable to complement the hypersensitivity. Protein–protein interaction between Xrn1p and tubulin would most likely depend on surface contacts and not depend on the enzymatic activity of Xrn1p. Since at least some of the *xrn1* point mutants described here likely alter residues within the active site of the enzyme and may not perturb other activities or structure of the protein, the lack of complementation strongly suggests that the putative interaction with tubulin is indirect. That these mutants do not greatly perturb protein structure is supported by the fact that they still display growth inhibition when overexpressed. An indirect connection between Xrn1p and tubulin is also suggested by the finding that mislocalization of a second exoribonuclease, Rat1p, from the nucleus to the cytoplasm complements benomyl hypersensitivity (17).

ACKNOWLEDGEMENTS

We would like to thank M.Burkart and Y.Xue for assistance in plasmid construction and S.Ross for help with the point mutation screen. We thank P.Ljundahl for providing a series of *xrn1* deletions prepared for sequence analysis, S.Peltz for providing plasmid DNA and DuPont for kindly providing benomyl. This work was supported in part by NIH fellowship grant GM13594 to A.J., NIH grant GM53655 to A.J. and NIH grant GM29383 to R.K.

REFERENCES

1 Larimer,F.W., Hsu,C.L., Maupin,M.K. and Stevens,A. (1992) *Gene*, **120**, 51–57.
2 Decker,C.J. and Parker,R. (1994) *Trends Biochem. Sci.*, **19**, 336–340.
3 Muhlrad,D. and Parker,R. (1994) *Nature*, **370**, 578–581.
4 Kim,J., Ljungdahl,P.O. and Fink,G.R. (1990) *Genetics*, **126**, 799–812.
5 Hsu,C.L. and Stevens,A. (1993) *Mol. Cell. Biol.*, **13**, 4826–4835.
6 Muhlrad,D., Decker,C.J. and Parker,R. (1994) *Genes Dev.*, **8**, 855–866.
7 Muhlrad,D., Decker,C.J. and Parker,R. (1995) *Mol. Cell. Biol.*, **15**, 2145–2156.
8 Stevens,A., Hsu,C.L., Isham,K.R. and Larimer,F.W. (1991) *J. Bacteriol.*, **173**, 7024–7028.
9 Stevens,A. (1980) *J. Biol. Chem.*, **255**, 3080–3085.
10 Decker,C.J. and Parker,R. (1993) *Genes Dev.*, **7**, 1632–1643.
11 Poole,T.L. and Stevens,A. (1997) *Biochem. Biophys. Res. Commun.*, **235**, 799–805.
12 Liu,Z. and Gilbert,W. (1994) *Cell*, **77**, 1083–1092.
13 Szankasi,P. and Smith,G.R. (1996) *Curr. Genet.*, **30**, 284–293.
14 Bashkirov,V.I., Scherthan,H., Solinger,J.A., Buerstedde,J.M. and Heyer,W.D. (1997) *J. Cell Biol.*, **136**, 761–773.
15 Shobuike,T., Sugano,S., Yamashita,T. and Ikeda,H. (1997) *Gene*, **191**, 161–166.
16 Heyer,W.-D., Johnson,A.W., Reinhart,U. and Kolodner,R.D. (1995) *Mol. Cell. Biol.*, **15**, 2728–2736.
17 Johnson,A.W. (1997) *Mol. Cell. Biol.*, **17**, 6122–6130.
18 Sugano,S., Shobuike,T., Takeda,T., Sugino,A. and Ikeda,H. (1994) *Mol. Gen. Genet.*, **243**, 1–8.
19 Shobuike,T., Sugano,S., Yamashita,T. and Ikeda,H. (1995) *Nucleic Acids Res.*, **23**, 357–361.
20 Kipling,D., Tambini,C. and Kearsey,S.E. (1991) *Nucleic Acids Res.*, **19**, 1385–1391.
21 Tishkoff,D.X., Rockmill,B., Roeder,G.S. and Kolodner,R.D. (1995) *Genetics*, **139**, 495–509.
22 Interthal,H., Bellocq,C., Bähler,J., Bashkirov,V.I., Edelstein,S. and Heyer,W.-D. (1995) *EMBO J.*, **14**, 1057–1066.
23 Johnson,A.W. and Kolodner,R.D. (1995) *Mol. Cell. Biol.*, **15**, 2719–2727.
24 Masison,D.C., Blanc,A., Ribas,J.C., Carroll,K., Sonenberg,N. and Wickner,R.B. (1995) *Mol. Cell. Biol.*, **15**, 2763–2771.
25 Anderson,J. and Parker,R. (1998) *EMBO J.*, **17**, 1497–1506.
26 Rose,M.D., Winston,F. and Hieter,P. (1990) *Methods in Yeast Genetics*. Cold Spring Harbor Laboratory Press, Cold Spring Harbor, NY.
27 Kranz,J.E. and Holm,C. (1990) *Proc. Natl. Acad. Sci. USA*, **87**, 6629–6633.
28 Tishkoff,D.X., Johnson,A.W. and Kolodner,R.D. (1991) *Mol. Cell. Biol.*, **11**, 2593–2608.
29 Johnson,A.W. and Kolodner,R.D. (1991) *J. Biol. Chem.*, **266**, 14046–14054.
30 Peltz,S.W., Brown,A.H. and Jacobson,A. (1993) *Genes Dev.*, **7**, 1737–1754.
31 Richardson,C.C. (1966) *J. Mol. Biol.*, **15**, 49–61.
32 Schatz,P.J., Solomon,F. and Botstein,D. (1988) *Mol. Cell. Biol.*, **6**, 3722–3733.
33 Bernard,L., Carroll,K., Valle,R.C.P. and Wickner,R.B. (1998) *Mol. Cell. Biol.*, **18**, 2688–2696.
34 Beese,L.S. and Steitz,T.A. (1991) *EMBO J.*, **10**, 25–33.
35 Mueser,T.C., Nossal,N.G. and Hyde,C.C. (1996) *Cell*, **85**, 1101–1112.
36 Xu,Y., Derbyshire,V., Ng,K., Sun,X.C., Grindley,N.D.F. and Joyce,C.M. (1997) *J. Mol. Biol.*, **268**, 284–302.
37 Amberg,D.C., Goldstein,L.A. and Cole,C.N. (1992) *Genes Dev.*, **6**, 1173–1189.